Recent and future changes of the Arctic sea-ice cover

Lars H. Smedsrud,[1] Asgeir Sorteberg,[1] and Kjell Kloster[2]

Received 28 May 2008; revised 8 August 2008; accepted 4 September 2008; published 23 October 2008.

[1] The present and future state of the Arctic sea ice cover is explored using new observations and a coupled one dimensional air–sea–ice model. Updated satellite observations of Fram Strait ice-area export show an increase over the last four years, with ~37% increase in winter 07–08. Atmospheric poleward energy flux declined since 1990, but advection of oceanic heat has recently increased. Simulations show that the ice area export is a stronger driver of thinning than the estimated ocean heat fluxes of 40 TW. Increased ocean heat transport will raise primarily Atlantic layer temperature. The 'present 2007' state of the Arctic ice could be a stable state given the recent high ice area export, but if ocean heat advection and ice export decrease, the ice cover will recover. A 2*CO_2 scenario with export and oceanic heat flux remaining strong, forecasts a summer Arctic open ocean area of 95% around 2050. **Citation:** Smedsrud, L. H., A. Sorteberg, and K. Kloster (2008), Recent and future changes of the Arctic sea-ice cover, *Geophys. Res. Lett.*, *35*, L20503, doi:10.1029/2008GL034813.

1. Introduction

[2] The interest in the Arctic sea ice seems inversely proportional to the area covered, and has exploded after the record minimum September 2007. The Arctic ice has in many ways become the ''canary in the coal mine'' of global warming. At the same time global models show a large spread in future predictions of the Arctic energy budget [*Sorteberg et al.*, 2007].

[3] The Arctic ice loss over the last few years has been well documented [*Nghiem et al.*, 2007; *Maslanik et al.*, 2007], but the causes of this major change have yet to be established. Furthermore, the idea that the Arctic may transfer into a seasonal ice cover within a limited number of years has gained large public interest. Here we use a physical process-based 1-D coupled air–sea–ice model to compare some key drivers of Arctic sea ice changes with updated trends, and find a fairly robust ice cover.

[4] Section 2 presents atmospheric energy transport from reanalysis data, estimates of heat advected north in the ocean, and new observations on Fram Strait ice-area export. Model simulations in section 3 show the effect over 10 years of these changes, and due to increased downward long-wave radiation caused by rising CO_2 concentrations. Initial conditions for the Arctic sea ice representing the 1960s and 2007 conditions are used.

[1]Bjerknes Centre for Climate Research, University of Bergen, Bergen, Norway.
[2]Nansen Environmental and Remote Sensing Center, Bergen, Norway.

0094-8276/08/2008GL034813

2. Recent Trends

2.1. Atmospheric Energy Transport

[5] Atmospheric energy transport to the Arctic increased until the 1990s, and was probably a major driver of the observed thinning [*Yu et al.*, 2004]. *Söderkvist and Björk* [2004] reproduced a thinning of 1.2 m up to the 1990s from the earlier 3.2 m mean based on this increase in atmospheric heat transport and cloud observations from the Russian drift stations. For the last 20 years there has been no increase in the overall northward atmospheric energy transport of the National Center for Environmental Prediction (NCEP) reanalysis [*Kalnay et al.*, 1996]; in fact the trend is slightly negative (Figure 1a).

[6] This result seems contradictory to the recent findings that the atmospheric energy transport drives a large portion of the Arctic warming [*Graversen et al.*, 2008]. However, they discuss trends for 1960–2001 and largely miss the recent change in trend. Focusing on a longer period, the linear annual trend (1956–2006) in our estimates (Figure 1a) is positive.

2.2. Oceanic Heat Transport

[7] The most recent estimate of oceanic heat transport to the Arctic in the Fram Strait [*Schauer et al.*, 2004] cover 1997–1999 and vary between 28 and 46 TW (10^{12} W). Distributing the heat over the Arctic Ocean area (using an area of 7.8×10^{12} m^2, the area deeper than 200 m, excluding the Barents and Kara Seas) gives a heat flux of 3.5–5.9 W/m^2. Historical estimates indicate a range of 18–67 TW for Fram Strait oceanic heat transport [*Simonsen and Haugan*, 1996]. Most of the inflow occurs between 100 and 400 m depth, and uncertainties are partly related to south-flowing water of Atlantic origin at greater depth.

[8] Further south in the Nordic Seas, a longer time series indicates a substantial and recent increase in northward advection of heat from 130 TW to 200 TW between 2004 and 2006 [*Skagseth et al.*, 2008]. This increase partly flows into the Barents Sea where a similar trend shows a doubling from roughly 40 TW to 80 TW. Although uncertain, the present understanding is that the Barents branch will lose most of its extra heat before entering the Arctic Ocean [*Simonsen and Haugan*, 1996]. These oceanic heat flux estimates use 0°C as reference temperature, roughly comparable to the returning overflow temperature across the Greenland-Scotland ridge.

[9] The Bering Strait heat flux likely doubled from ~4 TW to ~9 TW between 2001 and 2004 [*Woodgate et al.*, 2006]. The salinity of this inflow (~32.2) makes this water settle close to the mixed layer, and has a possible direct effect on the ice cover, as opposed to heat in the Atlantic Layer that arrives at a greater depth and needs to be mixed upwards. An increase in oceanic heat transport of 40 TW (5 W/m^2) will be discussed later, and compares to

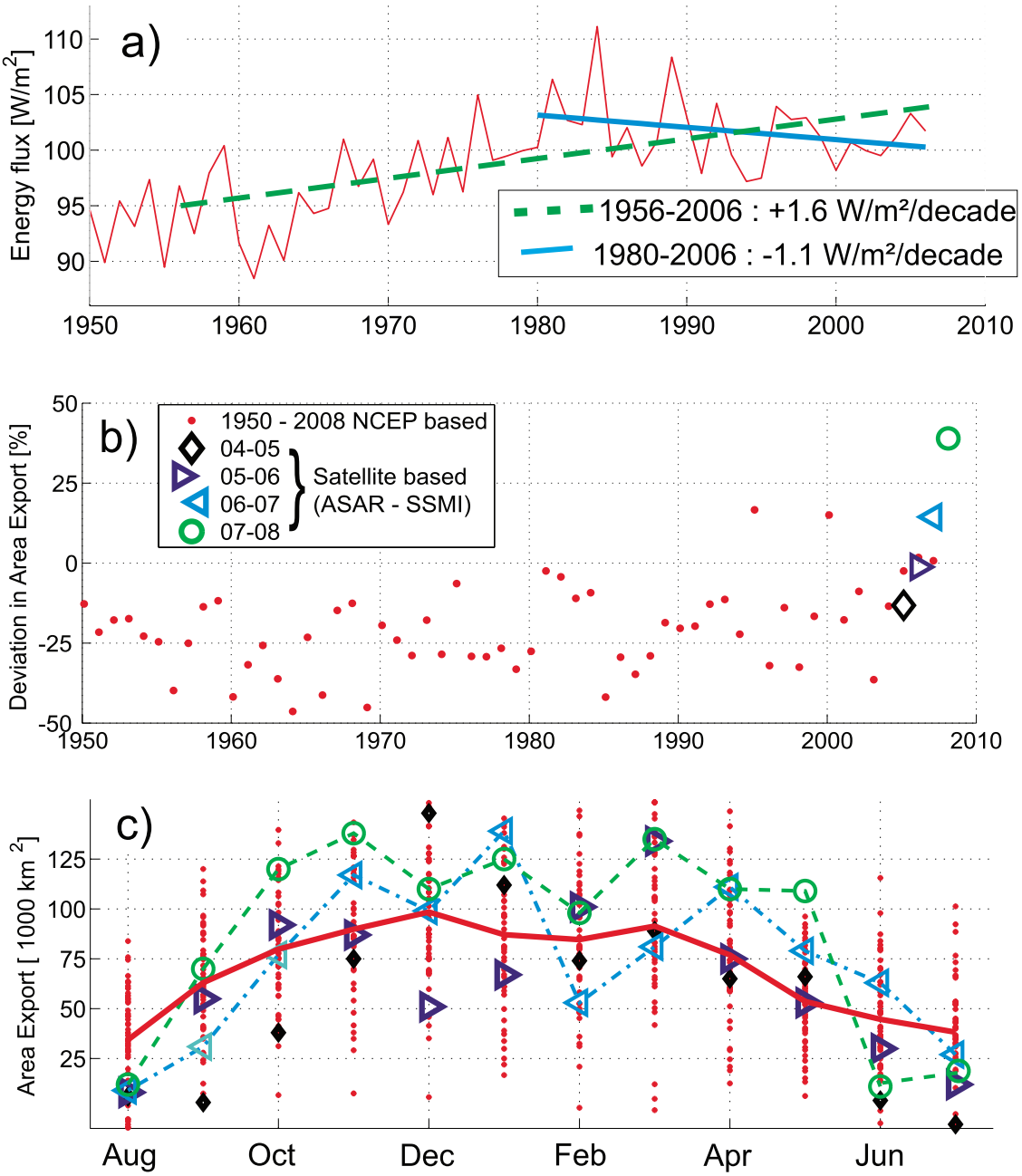

Figure 1. (a) The atmospheric energy flux towards the Arctic across 70°N calculated from NCEP reanalysis data. (b) The yearly Fram Strait ice area export. Values are plotted as deviation from the 2004–2007 mean; ASAR-SSMI mean is 774 × 10^3 km^2, NCEP reanalysis air pressure difference [*Widell et al.*, 2003] mean is 1095 × 10^3 km^2. (c) Monthly mean ice area export. The pressure based values are included in red (mean yearly cycle is solid line).

the long term change of the atmospheric heat transport between the 1960s and the 1990s in Figure 1a.

2.3. Fram Strait Ice Export

[10] The Fram Strait ice export varies substantially from month to month, and from year to year, but no obvious long-term trend has been visible so far [*Widell et al.*, 2003]. The maximum monthly ice-area flux is about 100 10^3 km^2 and occurs between December and March, while the minimum export usually occurs in August and July [*Kwok et al.*, 2004]. Figure 1 also presents new measurements from August 2004 through July 2008. Ice motion is calculated from ice feature displacement between two Envisat ASAR WideSwath images every 3 days. Ice concentration is based on the Norsex algorithm used on DMSP F13 SSMI brightness temperature data. The two data sets are combined to give the ice-area flux in subsequent 3-day periods, giving flux accuracy uncertainties over longer time periods (months) well below 10%.

[11] Estimates based on 1950–2008 NCEP reanalysis [*Kalnay et al.*, 1996] air pressure differences across the Fram Strait using the method of *Widell et al.* [2003] are

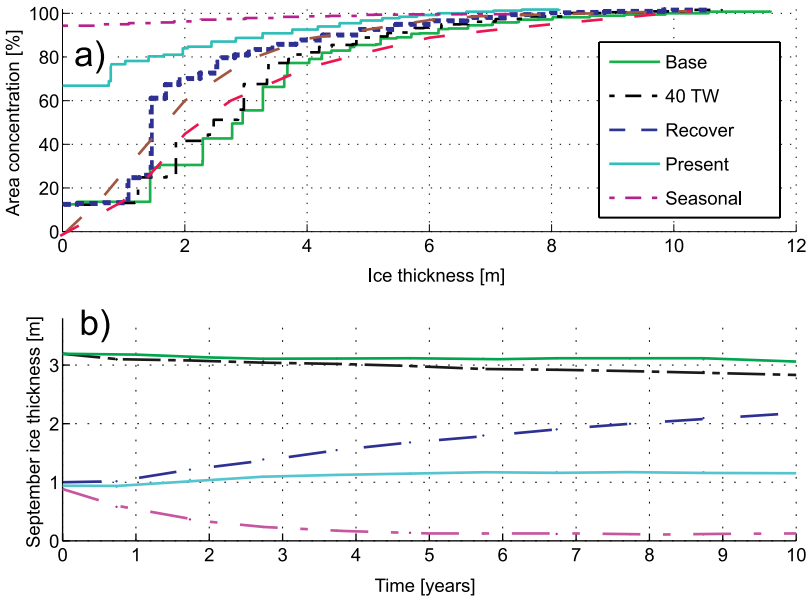

Figure 2. (a) Cumulative sea ice thickness distributions for the Arctic Ocean in summer. Submarine thickness observations from the 1960s (red dashed line) and the 1990s (brown dashed line) are included with the different model scenarios. The model distributions are results of 10 years with the different forcings. (b) The Arctic Ocean area averaged ice thickness in September under different scenarios.

included in Figure 1. The seasonal cycle of the 2004–2008 data compares well with the 1950–2000 mean cycle from *Widell et al.* [2003] (Figure 1c) and *Kwok et al.* [2004] (not shown). Figures 1b and 1c show that the ice area export has been high after 2003. However, it is only during 07–08 it has been higher than any other previous year since 1950. Updated through July 2008, the export is ~37% higher than for the last three years. For 06–07 the export was also high, but comparable to a few earlier winters.

[12] A large area export will decrease the Arctic sea-ice thickness and area. *Nghiem et al.* [2007] suggested that an increased export during winter 05–06 could explain the reduced 2006 ice cover. We find that winter 05–06 only had a moderately high export, comparable to some winters around 1980. The high export in January, April, May and June 2007 on the other hand (Figure 1c) would have contributed significantly to the September 2007 minimum.

[13] The 1950–2000 monthly mean area export is 73 × 10^3 km^2, equal to a yearly mean of 873 × 10^3 km^2 (Figure 1c). 07–08 had a higher export than indicated by the wind forcing. This was primarily caused by greater speed (not larger ice area), and is consistent with a thinner ice cover with less internal ice stresses. It is also consistent with a faster underlying ocean current, possibly speeding up geostrophically as a consequence of more melt-water.

3. Model Simulations

[14] 1DICE couples the horizontally averaged Arctic ice thickness distribution to the ocean and atmospheric columns [*Björk*, 1997]. The model resolves major processes like ice-albedo feedback, and is forced by monthly mean observations like horizontal atmospheric energy flux and short-wave radiation. Details on the forcing used in the Base (reference) simulation here are described by *Björk and Söderkvist* [2002], including a monthly varying Arctic ice divergence based on Fram Strait ice area export. The integrated ice thickness distribution is close to the submarine data [*Yu et al.*, 2004] (Figure 2a).

[15] *Björk and Söderkvist* [2002] showed that in steady state, 1DICE makes the Arctic sea ice seasonal at atmospheric energy transports above 110 W/m^2. As shown in Figure 1a is there no increase in atmospheric energy transport after 1990, and we thus find it unlikely that it has been a major contributor to recent ice reductions. We use a mean value of 103 W/m^2 for all simulations below. Unless otherwise specified we discuss changes over 10 years from the mean area averaged thickness of 3.1 m in the 'Base' simulation. The variation during a year is normally ~0.5 m, but we discuss the minimum thickness occurring in September (Figure 2b).

3.1. Sensitivity to Ocean Heat Advection and Mixing

[16] In section 2 we found a possible increase of oceanic heat transport below the Arctic sea ice. The magnitude remains open to speculation, but 40 TW of oceanic heat is a reasonable upper limit. About 5.5 TW of this additional heat would enter through the Bering Strait (above 50 m depth) as estimated by *Woodgate et al.* [2006], while the remaining 34.5 TW would enter through the Fram Strait (deeper than 50 m).

[17] The '40 TW' simulation is equal to 'Base' with 40 TW of oceanic heat spread equally down to 350 m depth. The main simulated effect on the ice cover is to increase the heat flux to the ice from below from about 1 to 2 W/m^2 in winter, compared to holding the Atlantic layer temperature fixed at 1.5°C at 350 m depth [*Björk and Söderkvist*, 2002]. This can be compared to the main heat flux reaching the model ice from below which is the solar heating of the mixed layer peaking at ~17 W/m^2 in summer. The additional advected heat decrease the mean ice thickness

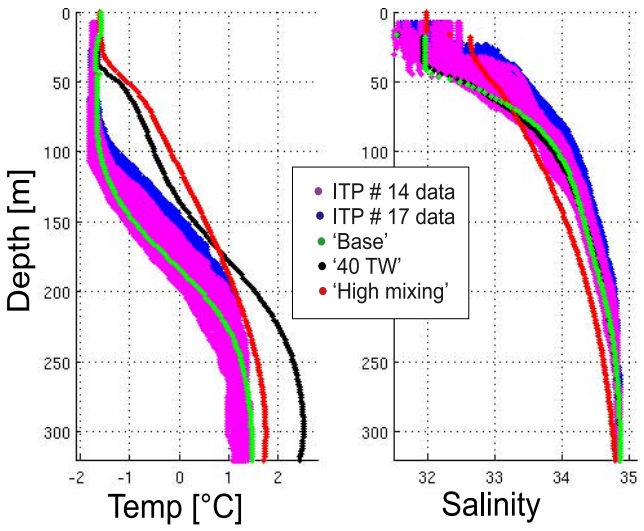

Figure 3. Temperature and salinity profiles from the Arctic Ocean. Ice-Tethered Profiler (ITP) data is plotted from two buoys drifting across most of the Eurasian Basin towards the Fram Strait (14 and 17, www.whoi.edu/itp) in 2007 and 2008. Model results are plotted at 10 years.

by 0.35 m as shown in Figure 2b. The above results are very similar to calculations of oceanic heat based on long term Arctic platforms [*Krishfield and Perovich*, 2005].

[18] Increasing the oceanic heat advection above 40 TW also increases the heat flux to the ice, but only modestly. Data show a slight warming below 100 m depth compared to the 'Base' temperature profile (Figure 3). Between 100 and 200 m it is similar in magnitude to the '40 TW' profiles at this depth.

[19] Excluding solar heating of the mixed layer, the heat reaching the ice from below is controlled by upward mixing of warmer deeper water. The upper 300 m of the Arctic water column is very stable, controlled by the fresher surface layer and the gradual increase in salinity towards the Atlantic core (Figure 3). Data from the pycnocline around the North Pole in April 2004–2007 (I. Fer, personal communication, 2008) occasionally indicate vertical diffusion being as high as $K_z \sim 20 \times 10^{-6}$ m^2/s, but usually the standard model value of $K_z = 2 \times 10^{-6}$ m^2/s is representative.

[20] Using the maximum estimate for K_z 1.0 m of ice is lost in 10 years instead of the 0.35 m ice loss in the '40 TW' case. The resulting ocean profiles are included in Figure 3 as the 'High mixing' case. This large vertical diffusion mixes the fresher colder surface with the warmer saltier Atlantic layer quite effectively, and removes the cold halocline (Figure 3). However, there is no sign of such a change in recent years. The cold halocline was missing for a region of the Eurasian Basin during the 1990s but has reappeared since then [*Björk et al.*, 2002].

[21] Profiles across the European Basin (between the North Pole and the Siberian coast) onwards from August 2007 show a 100 m deep column at the freezing point with a gradual increase in salinity (Figure 3). No clear signs of increased vertical mixing in the Arctic Ocean can thus be found in the observations. Diffusivity as high as $K_z \sim 20 \times 10^{-6}$ m^2/s might appear locally, or temporarily, but available ocean profiles indicate a mean diffusivity not larger than $K_z \sim 5 \times 10^{-6}$ m^2/s. Our calculations thus imply that the increased oceanic heat transport, working over 10 years, may be responsible for an ice reduction of 0.35–0.5 m depending on mixing.

3.2. CO_2 Forcing and Recent Changes

[22] The present ongoing global warming leads to increased long-wave radiation, and the water vapour feedback increases this radiation further. In the SRES A1B scenario the IPCC models show an increased incoming long-wave radiation of 30 W/m^2, compensated by a 10 W/m^2 reduction in incoming solar radiation due to more clouds at the end of the century [*Sorteberg et al.*, 2007].

[23] 1DICE does not include feedbacks related to changes in water vapour and clouds, but is forced by observed incoming solar radiation and calculates long-wave radiation based on optical thickness, N. A doubling of CO_2 can be simulated by increasing N by 7% [*Myhre et al.*, 1998]. This leads to an increased downward long-wave radiation from the normal value of 205 W/m^2 to 225 W/m^2, reducing the Arctic Ocean over 30 years to 80% open water and a 1.0 m horizontally averaged ice thickness.

[24] The September 2007 ice extent was the historical Arctic minimum in modern times [*Maslanik et al.*, 2007]. To explore the onwards development, we initialize the model scenarios with the following 2007 estimate; 40% open water and 60% ice concentration (20% 0.5 m, 20% 1.0 m, 10% 2.0 m, 5% 3.0 m and 5% 4.0 m). This creates a mean thickness close to 1.0 m. Present-day radiative forcing is used in the 'Recover' simulation (increasing N with 3.5%), giving a ~5 W/m^2 increase in downward long-wave radiation, otherwise it is equal to the 'Base' case. The resulting ice cover is not dependent on the initial ice condition in steady state. The response over 10 years is shown as the 'Recover' scenario in Figure 2, indicating a possible future increase in area averaged thickness to 2.2 m.

[25] As discussed above, the Arctic is presently experiencing an increased ice export and an increased oceanic advection of heat. The 'Present' scenario is forced by a 37% increase for all months in the prescribed mean monthly ice export, 40 TW added oceanic heat, and the 3.5% increase in N. The resulting thickness distribution has ~70% open water in summer, 10% 1 m thick ice, and a September ice thickness of 1.2 m (Figure 2b). The yearly cycle is enhanced compared to other simulations (not shown). With this ice cover and the increased optical thickness the downward long-wave radiation stabilises at 215 W/m^2, an increase of 10 W/m^2. The ice export is a stronger driver than the added oceanic heat. Without the increased ice export the ice recovers to 1.8 m in 10 years, but without the 40 TW the ice recovers to 1.5 m (not shown).

[26] The ongoing increase of greenhouse gases points to a realisation of radiative forcing comparable to a 2*CO_2 scenario in 2050. Should the Fram Strait ice export and oceanic advection remain as high as in the 'Present' simulation until 2050, the Arctic ice cover will be further reduced. The 'Seasonal' scenario includes the 'Present' forcing with the increased optical thickness caused by the 2*CO_2 forcing. This removes almost all remaining ice in 10 years. Figure 2a show that there is 95% open water, and none of the 12 remaining thickness classes holds more than

0.3% of the area. An increased ice export makes the transfer quicker, but it is the advection of 40 TW of oceanic heat that removes the Arctic summer ice completely.

4. Concluding Remarks

[27] Oceanic heat advection contributes to the ongoing reduction of the Arctic ice cover, but the increased ice-area export contributes more. Recent ocean profiles indicates no intensification in upward mixing of heat from the Atlantic layer (Figure 3). Advection of atmospheric heat has also decreased slightly during the last 20 years, and thus cannot account for the present ongoing dramatic changes (Figure 1a).

[28] It is beyond the scope of this paper to discuss the dynamical changes leading to the recent anomalies in oceanic heat transport and ice export. Regional differences within the Arctic Ocean, changes in cloud cover and ridging/rafting efficiency are not addressed either. An anomalous Arctic meridional circulation has persisted since 2000 [*Overland et al.*, 2008], quite similar to the Arctic dipole anomaly found to have a major influence on Arctic sea ice motion in general [*Wu et al.*, 2006].

[29] Our model results show that the 2007 minimum could be maintained by high Fram Strait ice export and oceanic heat advection, but a further increase in forcing, like a $2*CO_2$ state, is needed to drive the Arctic into a seasonal ice free cover permanently. As the globe slowly warms, the Arctic ice cover will slowly diminish too, but there are limits as to how fast this can take place. This depends on Arctic cloud cover as much as it does on greenhouse gas forcing. The increased Fram Strait ice export reported here forecasts a reduced ice cover also in 2008, but if the present high export is not maintained it is likely that we will see a partly recovery in the next few years. The low June 2008 export (Figure 1c) may have a significant effect on the September 2008 minimum.

[30] **Acknowledgments.** For Lars H. and Asgeir this work was completed as a part of the POCAHONTAS and NorClim projects funded by the Research Council of Norway. Kjell was supported by the MERSEA and DAMOCLES projects. The Ice-Tethered Profiler data were collected and made available by the Ice-Tethered Profiler Program based at the Woods Hole Oceanographic Institution (http://www.whoi.edu/itp). Thanks to M.L. Timmermans, T. Eldevik, and A. Wåhlin for valuable comments, and G. Björk for the 1DICE model. The SAR images were delivered by the European Space Agency (ESA). This is publication A197 from the Bjerknes Centre for Climate Research.

References

Björk, G. (1997), The relation between ice deformation, oceanic heat flux, and the ice thickness distribution in the Arctic Ocean, *J. Geophys. Res.*, *102*, 18,689–18,698.

Björk, G., and J. Söderkvist (2002), Dependence of the Arctic Ocean ice thickness distribution on the polward energy flux in the atmosphere, *J. Geophys. Res.*, *107*(C10), 3173, doi:10.1029/2000JC000723.

Björk, G., J. Söderkvist, P. Winsor, A. Nikolopoulus, and M. Steele (2002), Return of the cold halocline layer to the Amundsen Basin in the Arctic Ocean: Implications for sea ice mass balance, *Geophys. Res. Lett.*, *29*(11), 1513, doi:10.1029/2001GL014157.

Graversen, R., T. Mauritsen, M. Tjernström, E. Källen, and G. Svensson (2008), Vertical structure of recent Arctic warming, *Nature*, *541*, 53–56, doi:10.1038/nature06502.

Kalnay, E., et al. (1996), The NCEP/NCAR 40-year reanalysis project, *Bull. Ame. Meteorol. Soc.*, *77*, 437–471.

Krishfield, R., and D. Perovich (2005), Spatial and temporal variability of oceanic heat flux to the Arctic ice pack, *J. Geophys. Res.*, *110*, C07021, doi:10.1029/2004JC002293.

Kwok, R., G. Cunningham, and S. Pang (2004), Fram Strait sea ice outflow, *J. Geophys. Res.*, *109*, C01009, doi:10.1029/2003JC001785.

Maslanik, J., C. Fowler, J. Stroeve, S. Drobot, J. Zwally, D. Yi, and W. Emery (2007), A younger, thinner Arctic ice cover: Increased potential for rapid, extensive sea-ice loss, *Geophys. Res. Lett.*, *34*, L24501, doi:10.1029/2007GL032043.

Myhre, G., E. Highwood, K. Shine, and F. Stordal (1998), New estimates of radiative forcing due to well mixed greenhouse gases, *Geophys. Res. Lett.*, *25*, 2715–2718.

Nghiem, S., I. Rigor, D. Perovich, P. Clemente-Colon, J. Weatherly, and G. Neumann (2007), Rapid reduction of Arctic perennial sea ice, *Geophys. Res. Lett.*, *34*, L19504, doi:10.1029/2007GL031138.

Overland, J., M. Wang, and S. Salo (2008), The recent Arctic warm period, *Tellus, Ser. A*, *60*, 589–597, doi:10.1111/j.1600-0870.2008.00327.x.

Schauer, U., E. Fahrbach, S. Østerhus, and G. Rohardt (2004), Arctic warming through the Fram Strait: Oceanic heat transport from 3 years of measurements, *J. Geophys. Res.*, *109*, C06026, doi:10.1029/2003JC001823.

Simonsen, K., and P. M. Haugan (1996), Heat budgets for the Arctic Mediterranean and sea surface heat flux parameterizations for the Nordic Seas, *J. Geophys. Res.*, *101*, 6553–6576.

Skagseth, Ø., T. Furevik, R. Ingvaldsen, H. Loeng, K. Mork, K. Orvik, and V. Ozhigin (2008), Volume and heat transport to the Arctic Ocean via the Norwegian and Barents Seas, in *Arctic-Subarctic Ocean Fluxes*, edited by R. Dickson, J. Meincke, and P. Rhines, pp. 45–64, Springer, New York.

Söderkvist, J., and G. Björk (2004), Ice thickness variability in the Arctic Ocean between 1954–1990 results from a coupled ocean-ice-atmosphere column model, *Clim. Dyn.*, *22*, 57–68, doi:10.1007/s00382-003-0363-z.

Sorteberg, A., V. Kattsov, J. Walsh, and T. Pavlova (2007), The Arctic surface enrgy budget as simulated with the IPCC AR4 AOGCMs, *Clim. Dyn.*, *29*, 131–156, doi:10.1007/s00382-006-0222-9.

Widell, K., S. Østerhus, and T. Gammelsrød (2003), Sea ice velocity in the Fram Strait monitored by moored instruments, *Geophys. Res. Lett.*, *30*(19), 1982, doi:10.1029/2003GL018119.

Woodgate, R., K. Aagaard, and T. Weingartner (2006), Interannual changes in the Bering Strait fluxes of volume, heat and freshwater between 1991 and 2004, *Geophys. Res. Lett.*, *33*, L15609, doi:10.1029/2006GL026931.

Wu, B., J. Wang, and J. Walsh (2006), Dipole anomaly in the winter Arctic atmosphere and its association with sea ice motion, *J. Clim.*, *19*, 210–225.

Yu, Y., G. Maykut, and D. Rothrock (2004), Changes in the thickness distribution of Arctic sea ice between 1958–1970 and 1993–1997, *J. Geophys. Res.*, *109*, C08004, doi:10.1029/2003JC001982.

K. Kloster, Nansen Environmental and Remote Sensing Center, N-5037 Bergen, Norway.

L. H. Smedsrud and A. Sorteberg, Bjerknes Centre for Climate Research, University of Bergen, Allegaten 70, N-5007 Bergen, Norway. (larsh@gfi.uib.no)